BNL-HET-99/36
TTP99-46
October 1999
hep-ph/9910496

Asymptotic Expansions — Methods and Applications *

Robert Harlander

HET, Physics Department, Brookhaven National Laboratory, Upton, NY 11973

Different viewpoints on the asymptotic expansion of Feynman diagrams are reviewed. The relations between the field theoretic and diagrammatic approaches are sketched. The focus is on problems with large masses or large external momenta. Several recent applications also for other limiting cases are touched upon. Finally, the pros and cons of the different approaches are briefly discussed.

PACS numbers: 12.38.Bx, 11.80.Fv, 13.65.+i

1. Introduction

Feynman diagrams are the most important theoretical tool for particle physicists. They are an efficient link between theory and experiment. However, their translation into actual numerical predictions is often very tedious if not impossible. Huge efforts have been devoted to their evaluation, and several powerful methods have been developed to systemize their treatment. The more complex a Feynman diagram is, the more important is it to find approximation procedures that allow to solve the problem with finite but reasonable accuracy. In this paper we will describe methods that have been developed over the recent years in order to systematically expand Feynman diagrams in their external parameters.

2. Status of multi-loop calculations

The complexity of a Feynman diagram with a certain number of loops mainly depends on its number of scales (i.e., masses and external momenta). In the one-loop case, the problem can be considered as solved. Any tensor integral can be reduced to integrals of unit numerator which have been studied extensively. Nowadays there are powerful software tools, on the

* Presented at the XXIII School of Theoretical Physics, Ustroń99.

one hand concerned with the tensor reduction, on the other hand with the numerical or analytical evaluation of the integrals (see, e.g., [1]).

At two-loop level the solution is not as general as in the one-loop case. However, the important class of two-point functions is well under control, and the development for three- and four-point functions is under continuous progress (see [2] for a list of references).

Therefore, two-loop calculations in theories like the electro-weak standard model and even in supersymmetric models whose particle spectra give rise to Feynman diagrams with several different scales have become feasible (e.g. [3]).

Calculations at three-loop level mostly reside on two different classes of analytically solvable Feynman integrals. These two classes are

- massless propagator-type diagrams where all internal lines are massless and only one external momentum is different from zero. Schematically:

$$I(n_1,\ldots,n_\alpha) = \int \mathrm{d}^D k_1 \mathrm{d}^D k_2 \mathrm{d}^D k_3 \frac{P(q,k_1,k_2,k_3)}{(p_1^2)^{n_1}\cdots(p_\alpha^2)^{n_\alpha}}\,, \qquad (1)$$

  where α is the number of propagators and the p_i are linear combinations of the k_j and the external momentum q.

- massive tadpole diagrams not carrying any external momenta and internal lines being either massless or carrying a common mass m. Schematically:

$$J(n_1,\ldots,n_\alpha) = \int \mathrm{d}^D k_1 \mathrm{d}^D k_2 \mathrm{d}^D k_3 \frac{P(k_1,k_2,k_3)}{(m_1^2+p_1^2)^{n_1}\cdots(m_\alpha^2+p_\alpha^2)^{n_\alpha}}\,, \quad (2)$$

  where the m_i are either equal to zero or m, and the p_i are linear combinations of the loop momenta k_j.

$P(\ldots)$ is a polynomial of products of its arguments. The method how to solve such integrals is called the integration-by-parts algorithm [4]. It is based on identities derived from the fact that the D-dimensional integral over a total derivative is equal to zero:

$$\int \mathrm{d}^D p \, \frac{\partial}{\partial p_\mu} f(p,\ldots) = 0\,. \qquad (3)$$

These identities can be arranged in such a way that they yield recurrence relations that allow to reduce some of the "indices" $n_1,\ldots,n_\alpha$ in (1), (2) to zero. At three-loop level, these relations have been derived in [4] for massless propagators and in [5,6] for massive tadpole integrals. Their application to a general three-loop diagram may generate huge intermediate expressions that easily exceed several hundreds of megabytes on a computer. This is why one needs to implement the relations to powerful computer algebra systems like `FORM` or `REDUCE`. Two such implementations are `MINCER` [7], concerned with the massless propagator diagrams and `MATAD` [8], dealing with the massive tadpoles (see [2] for a review on automatic computation of Feynman diagrams).

The two classes of single-scale diagrams mentioned above already have a huge number of important applications. The most popular one probably is the total cross section for hadron production in e^+e^- annihilation (see, e.g., [9]), usually written as the hadronic R ratio, in the limit of vanishing quark masses. Using the optical theorem, it can be expressed through the imaginary part of the photon polarization function:

$$R(s) = 12\pi \mathrm{Im}\Pi(q^2)\bigg|_{q^2=s+i\epsilon}\,, \tag{4a}$$

$$\text{where} \qquad \Pi(q^2) = \frac{-g_{\mu\nu}+q_\mu q_\nu/q^2}{q^2(D-1)}\Pi_{\mu\nu}(q)\,, \tag{4b}$$

$$\text{and} \qquad \Pi_{\mu\nu}(q) = i\int \mathrm{d}^4x e^{iq\cdot x}\langle 0|\mathrm{T}j_\mu(x)j_\nu(0)|0\rangle\,, \qquad j_\mu = \bar\psi\gamma_\mu\psi\,. \tag{4c}$$

ψ is a quark field of mass m. The diagrams contributing to $\Pi_{\mu\nu}(q)$ up to two-loop order are shown in Fig. 1. Up to three-loop order, such diagrams can directly be computed by the program `MINCER` mentioned before (*nota bene* in the massless limit!). Another important application is the computation of moments of the polarization function, $\partial^n/\partial(q^2)^n \cdot \Pi(q^2)|_{q^2=0}$. They can be obtained by applying the derivatives and the nullification of q^2 *before* performing the loop integrations [10]. Furthermore, since renormalization group functions like the QCD β function or anomalous dimensions in the $\overline{\mathrm{MS}}$ scheme are independent of any masses and momenta, their evaluation can be performed by computing single-scale diagrams.

However, returning to the R ratio defined above, the limit of vanishing quark mass may not be satisfactory, especially if one is interested in energy regions not too far above one of the quark thresholds. As long as the exact evaluation of three-loop diagrams involving a non-vanishing mass as well as an arbitrary external momentum is not possible, one may hope to reduce the integrals to single-scale diagrams by performing an expansion in the quark mass. In the optimal case, a finite number of terms in the expansion will approximate the full result to reasonable accuracy, and the inclusion of higher order terms will gradually decrease the error. To get an idea on what the result should look like, let us consider the exact one-loop result

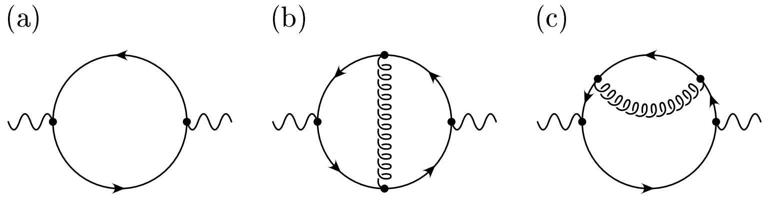

Fig. 1. Diagrams contributing to the photon polarization function $\Pi(q)$. The outer line denotes a photon of momentum q, the plain lines are quarks and the spiral ones denote gluons.

for the photon polarization function:

$$\Pi^{(0)}(q^2) = \frac{3}{16\pi^2}\left(\frac{4}{3\epsilon} + \frac{20}{9} + \frac{4}{3}\,l_{\mu m} + \frac{4}{3z} - \frac{4(1-z)(1+2z)}{3z}G(z)\right) ,$$

where (5)

$$G(z) = \frac{2u\ln u}{u^2-1}\,, \quad u = \frac{\sqrt{1-1/z}-1}{\sqrt{1-1/z}+1}\,, \quad z = \frac{q^2}{4m^2}\,, \quad l_{\mu m} = \ln\frac{\mu^2}{m^2}\,,$$

and μ is the renormalization scale. The pole[1] in $\epsilon = (D-4)/2$, where D is the space-time dimension, will eventually disappear upon global renormalization (e.g., by requiring $\Pi(0) = 0$). The result of (5) can be expanded in terms of small mass m, yielding:

$$\Pi^{(0)}(q^2) = \frac{3}{16\pi^2}\left\{\frac{4}{3\epsilon} + \frac{20}{9} - \frac{4}{3}\,l_{q\mu} + 8\,\frac{m^2}{q^2} + \left(\frac{m^2}{q^2}\right)^2\left[4 + 8\,l_{qm}\right]\right\} + \ldots\,, \tag{6}$$

with $l_{q\mu} = \ln(-q^2/\mu^2)$ and $l_{qm} = \ln(-q^2/m^2)$. One observes that the coefficients of the series in m^2/q^2 contain non-analytical pieces in terms of logarithms. They develop an imaginary part by means of

$$\ln(-s - i\epsilon) = -i\pi + \ln s \qquad \text{for } s > 0. \tag{7}$$

The hadronic R ratio is therefore given by (see (4a)):

$$R(s) = 3\left(1 - 6\left(\frac{m^2}{s}\right)^2 + \ldots\right) . \tag{8}$$

[1] The accompanying $\ln 4\pi$ and γ_{E} are suppressed throughout the paper.

The question is now if it is possible to obtain the expansion given in (6) directly from the Feynman integrals, i.e. without having to know the exact result. As a first guess one may try to perform a Taylor expansion of the integrand, thereby arriving at massless propagator diagrams. However, it is clear that such a "naive Taylor expansion" can not be the whole answer. For example, it is impossible to reproduce the logarithmic mass dependence in this way. Nevertheless, let us look at the result:

$$\begin{aligned} \mathcal{T}_m\Pi^{(0)} = \frac{3}{16\pi^2}\bigg\{ & \frac{4}{3\epsilon} + \frac{20}{9} - \frac{4}{3}l_{q\mu} \\ & + 8\,\frac{m^2}{q^2} + \left(\frac{m^2}{q^2}\right)^2\left[-\frac{8}{\epsilon} - 8 + 8\,l_{q\mu}\right]\bigg\} + \cdots . \end{aligned} \tag{9}$$

In fact, the first two orders in m^2/q^2 are reproduced correctly. The m^4/q^4 term, however, is completely different, and there is even an additional pole in ϵ. Only the logarithmic q^2 dependence is reproduced. Thus, in general the naive Taylor expansion is not sufficient to arrive at the desired result. However, in the next section we will see that by including well-defined additional terms one indeed can obtain the correct expansion.

3. Asymptotic Behavior

This section is divided into three parts, all concerned with the problem of expanding Feynman diagrams in their external parameters, as it was raised in Section 2. Cross-references between the three parts of this section will demonstrate the close correspondence of the individual formulations.

In Section 3.1, the problem will be approached from a field theoretical point of view. The resulting expansion will be derived from the operator product expansion formulated in the $\overline{\mathrm{MS}}$ scheme. The viewpoint of Section 3.2, on the other hand, examines the individual Feynman integrals that contribute to a certain problem. By a thorough investigation of the integration regions for the loop momenta and a subsequent Taylor expansion in the appropriate variables, one can derive rules that allow to obtain the expansion of the full result in a very efficient way.

In certain cases these rules could be phrased in a mainly diagrammatical language. For diagrams involving large external momenta or large masses this graphical formulation will be described in Section 3.3.

3.1. Operator Product Expansion

The asymptotic behavior of the two-point correlator of (4c) in the limit $-q^2 = Q^2 \to \infty$ is formally known to all orders of perturbation theory. It

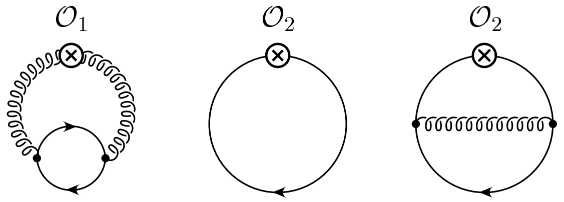

Fig. 2. Sample diagrams contributing to $\langle\mathcal{O}_1\rangle$ and $\langle\mathcal{O}_2\rangle$.

is given by an operator product expansion (OPE):

$$\Pi_{\mu\nu}(q) = i\int \mathrm{d}^4x e^{iq\cdot x}\langle 0|\mathrm{T}j_\mu(x)j_\nu(0)|0\rangle \stackrel{-q^2\to\infty}{\to} \sum_n C_{n,\mu\nu}\langle\mathcal{O}_n\rangle\,. \tag{10}$$

The $C_{n,\mu\nu}$ are complex functions, and the $\mathcal{O}_n$ are operators composite of fields of the QCD Lagrangian. We keep only Lorentz scalar operators because all others vanish when sandwiched between the vacuum states. Transversal coefficient functions C_n will be defined in analogy to the Eq. (4b). The operators are usually sorted according to their mass dimension. It is convenient to allow only operators of even mass dimension which is achieved by appropriate factors of the quark mass m (only one quark shall be considered as massive for the sake of clarity). Up to dimension four, the following set of operators is relevant:

$$\begin{aligned}&\mathcal{O}^{(0)} = \mathbf{1}\,, \qquad \mathcal{O}^{(2)} = \mathbf{m}^2\,,\\ &\mathcal{O}_1^{(4)} = G_{\mu\nu}^2\,, \quad \mathcal{O}_2^{(4)} = m\bar{\psi}\psi\,, \quad \mathcal{O}_3^{(4)} = \mathbf{m}^4\,,\end{aligned} \tag{11}$$

where $G_{\mu\nu}$ is the gluonic field strength tensor and ψ is again the quark field (the superscript "(4)" of the dimension-4 operators will be dropped in what follows). If the operators are understood to be normal ordered, the vacuum expectation values of the non-trivial (i.e. not proportional to unity) operators are equal to zero in perturbation theory. In such an approach these operators are used to parameterize non-perturbative effects (see, e.g., [11]).

On the other hand, if one abandons normal ordering and applies minimal subtraction, the vacuum expectation values of the field operators receive also perturbative contributions. The corresponding diagrams are massive tadpoles which by definition only depend on the quark mass and the renormalization scale μ. Examples are shown in Fig. 2. They lead to the following results:

$$
\begin{aligned}
\langle \mathbf{1} \rangle &= 1\,, \quad \langle \mathbf{m}^2 \rangle = m^2\,, \quad \langle \mathbf{m}^4 \rangle = m^4\,, \\
\langle \mathcal{O}_1^{\rm B} \rangle &= \frac{3}{16\pi^2}\, m^4 \left\{ \frac{\alpha_s}{\pi} \left[\frac{2}{\epsilon^2} + \frac{1}{\epsilon}\left(\frac{14}{3} + 4\, l_{\mu m}\right) \right.\right. \\
&\qquad \left.\left. + 10 + 2\,\zeta_2 + \frac{28}{3}\, l_{\mu m} + 4\, l_{\mu m}^2 \right] + \cdots \right\}, \\
\langle \mathcal{O}_2^{\rm B} \rangle &= \frac{3}{16\pi^2}\, m^4 \left\{ \frac{4}{\epsilon} + 4 + 4\, l_{\mu m} + \frac{\alpha_s}{\pi}\left[\cdots\right] + \cdots \right\}.
\end{aligned}
\tag{12}
$$

Only the first non-vanishing order in α_s is quoted here. However, the results for the operators that are proportional to unity ($\mathbf{m}^{2n}, n = 0, 1, 2$) are valid to all orders of perturbation theory by definition. Note that there are still poles in ϵ which is why the operators are marked with the superscript B. These poles disappear upon global renormalization, thereby inducing mixing of the operators according to

$$
\mathcal{O}_n = \sum_m Z_{nm} \mathcal{O}_m^{\rm B}\,. \tag{13}
$$

For the dimension-4 operators the renormalization matrix Z_{nm} in the $\overline{\rm MS}$ scheme was computed in [12] by expressing it in terms of the charge and mass renormalization constants of QCD, plus the one for the QCD vacuum energy. They are currently known to $\mathcal{O}(\alpha_s^4)$ [13,14] and $\mathcal{O}(\alpha_s^3)$ [15], respectively. The results for the renormalized vacuum expectation values of $\mathcal{O}_1$ and $\mathcal{O}_2$ up to $\mathcal{O}(\alpha_s)$ can be found in [16].

The crucial observation about using the $\overline{\rm MS}$ scheme was made in [17]: It appears that in this approach the coefficient functions are independent of the quark masses. They only depend on the external momentum q and the renormalization scale μ. It was shown that their computation can be reduced to the evaluation of massless propagator-type diagrams. The most refined method for this purpose is called the "method of projectors" [18]: let us define "bare" coefficient functions through

$$
\sum_n C_{n,\rm B} \mathcal{O}_n^{\rm B} \equiv \sum_n C_n \mathcal{O}_n\,. \tag{14}
$$

Then the ones up to dimension four, for example, are obtained in the following way (only sample diagrams are displayed here) [19]:

$$[C_{\rm B}^{(0)},\, C_{\rm B}^{(2)},\, C_{3,\rm B}] =$$

$$= [1,\ \frac{\partial}{\partial m_{\rm B}^2},\ \frac{1}{2}\frac{\partial^2}{\partial (m_{\rm B}^2)^2}] \Bigg[$$

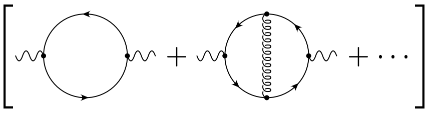

$$\Bigg]_{m_{\rm B}=0}\ ,$$

$$C_{1,\rm B} = \mathcal{P}_1\left(\frac{\partial}{\partial p}, \frac{\partial}{\partial m_{\rm B}}\right)\Bigg[$$

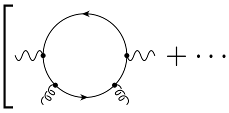

$$\Bigg]_{m_{\rm B}=p=0}\ ,$$

$$C_{2,\rm B} = \mathcal{P}_2\left(\frac{\partial}{\partial p}, \frac{\partial}{\partial m_{\rm B}}\right)\Bigg[$$

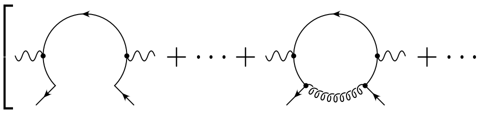

$$\Bigg]_{m_{\rm B}=p=0}\ , \tag{15}$$

where p is the momentum carried by the external quark-, gluon-, and ghost-lines (the latter arise only at higher orders in α_s). $\mathcal{P}_1$ and $\mathcal{P}_2$ are “projectors” depending polynomially on the derivatives w.r.t. p and $m_{\rm B}$. For example,

$$\mathcal{P}_2\left(\frac{\partial}{\partial p}, \frac{\partial}{\partial m_{\rm B}}\right)[\cdots] = \frac{1}{4n_c}{\rm Tr}\left(\frac{\partial}{\partial m_{\rm B}} + \frac{1}{D}\gamma^\nu\frac{\partial}{\partial p^\nu}\right)[\cdots]\,. \tag{16}$$

It is understood that the derivatives act on the *integrands* and the nullification of p and $m_{\rm B}$ is performed *before* integration. Note, however, that the momentum carried by the external currents (wavy lines), is $q \neq 0$. Obviously, $C_{\rm B}^{(0)}$, $C_{\rm B}^{(2)}$, and $C_{3,\rm B}$ are just the coefficients of $m_{\rm B}^0$, $m_{\rm B}^2$, and $m_{\rm B}^4$ of the naive Taylor expansion, respectively. The expressions for $C_{1,\rm B}$ and $C_{2,\rm B}$, on the other hand, read as follows:

$$\begin{aligned}
C_{1,\rm B} &= \frac{1}{q^4}\left\{\frac{\alpha_s}{\pi}\left[\frac{1}{12} + \epsilon\left(\frac{7}{72} - \frac{1}{12}l_{q\mu}\right)\right] + \ldots\right\},\\
C_{2,\rm B} &= \frac{1}{q^4}\left\{2 + \epsilon + \frac{\alpha_s}{\pi}\left[\frac{2}{3} + \epsilon\left(\frac{5}{3} - \frac{2}{3}l_{q\mu}\right)\right] + \ldots\right\},
\end{aligned} \tag{17}$$

where we have kept the terms up to $\mathcal{O}(\epsilon)$ because they contribute to the finite part of $\Pi(q^2)$. In fact, with these ingredients it is possible to compute the polarization function up to order $\alpha_s^0 m^4$. Diagrammatically one finds

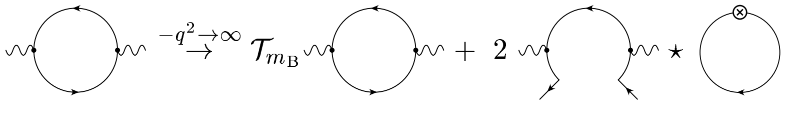

$$\tag{18}$$

where in the second term on the right hand side the projection with $\mathcal{P}_2$ from (16) is implicit. The factor 2 arises from the symmetrical diagram that also contributes to $C_{2,\mathrm{B}}$. Note that there is no contribution from $\mathcal{O}_1$ at this order. The Taylor expansion in the first term is to be carried out up to m_{B}^4. This first term is given by Eq. (9), since $m = m_{\mathrm{B}} + \mathcal{O}(\alpha_s)$. Using the results of (12) and (17) for $C_{2,\mathrm{B}}$ and $\langle \mathcal{O}_2^{\mathrm{B}} \rangle$, one obtains the result for the second term of (18):

$$2\, C_{2,\mathrm{B}} \langle \mathcal{O}_2^{\mathrm{B}} \rangle = \frac{3}{16\pi^2} \left(\frac{m^2}{q^2} \right)^2 \left[\frac{8}{\epsilon} + 12 + 8\, l_{\mu m} \right] + \mathcal{O}(\alpha_s)\,. \tag{19}$$

Adding it to (9) exactly reproduces the result for $\Pi(q^2)$ up to $\mathcal{O}(m^4)$ given in (6).

The conclusion from these considerations is that in addition to the naive Taylor expansion of (9) one should include an extra term, given by $2\, C_{2,\mathrm{B}} \langle \mathcal{O}_2^{\mathrm{B}} \rangle$, in order to arrive at the correct result for the polarization function. However, the important point about Eq. (18) is that the original diagram is reduced to single-scale factors (i.e., massless propagators and massive tadpoles).

3.2. Strategy of Regions [20, 21]

Let us for the moment forget about OPE again and consider only the Feynman integral for the one-loop diagram, concentrating on the scalar case for the sake of clarity:

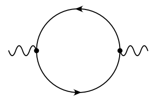

$$\overset{\text{scalar}}{=} \int \frac{1}{m^2 + k^2} \frac{1}{m^2 + (k-Q)^2}\,, \tag{20}$$

where the momenta are taken in Euclidean space and integration is over k. Assume now that $m^2 \ll Q^2\,(= -q^2)$. The integral may be split into the following regions:

$$\begin{array}{llll} (i): & k^2 \gg m^2 & \text{and} & (k-Q)^2 \gg m^2 \\ (ii): & k^2 \sim m^2 & \Rightarrow & (k-Q)^2 \gg m^2 \\ (iii): & (k-Q)^2 \sim m^2 & \Rightarrow & k^2 \gg m^2\,, \end{array} \tag{21}$$

where $\sim$ means "of the order of". In region (i), the integrand can be expanded in terms of small m:

$$\begin{aligned} &\int_{(i)} \frac{1}{m^2 + k^2} \frac{1}{m^2 + (k-Q)^2} \approx \int_{(i)} \mathcal{T}_m \frac{1}{m^2 + k^2} \frac{1}{m^2 + (k-Q)^2} = \\ &= \int_{(i)} \frac{1}{k^2} \frac{1}{(k-Q)^2} \left(1 - \frac{m^2}{k^2} + \ldots \right) \left(1 - \frac{m^2}{(k-Q)^2} + \ldots \right). \end{aligned} \tag{22}$$

In region (ii), k is considered to be of the same order of magnitude as m, so one should expand in m and k at the same time:

$$\begin{aligned}\int_{(ii)} \frac{1}{m^2+k^2}\frac{1}{m^2+(k-Q)^2} &\approx \int_{(ii)} \mathcal{T}_{m,k}\frac{1}{m^2+k^2}\frac{1}{m^2+(k-Q)^2} = \\ = \int_{(ii)} \frac{1}{m^2+k^2}\frac{1}{Q^2}&\left(1-\frac{m^2+k^2-2k\cdot Q}{Q^2}+\dots\right) .\end{aligned} \tag{23}$$

Region (iii) can be mapped onto region (ii) by substituting $k' = Q - k$, meaning $k'^2 \sim m^2 \Rightarrow (k'-Q)^2 \gg m^2$, and we arrive at an expression analoguous to (23).

Now we add and subtract the complementary regions to the integrals above and find:

$$\begin{aligned}&\int \frac{1}{m^2+k^2}\frac{1}{m^2+(k-Q)^2} \approx \\ &\approx \int \mathcal{T}_m\frac{1}{m^2+k^2}\frac{1}{m^2+(k-Q)^2} + 2\int \frac{1}{m^2+k^2}\mathcal{T}_{m,k}\frac{1}{m^2+(k-Q)^2} \\ &\quad - C ,\end{aligned} \tag{24}$$

where

$$\begin{aligned}C = &\int_{(ii)\cup(iii)} \mathcal{T}_m\frac{1}{m^2+k^2}\frac{1}{m^2+(k-Q)^2} + \int_{(i)\cup(iii)} \frac{1}{m^2+k^2} \times \\ &\times \mathcal{T}_{m,k}\frac{1}{m^2+(k-Q)^2} + \int_{(i)\cup(ii)} \frac{1}{m^2+k'^2}\mathcal{T}_{m,k'}\frac{1}{m^2+(k'-Q)^2} .\end{aligned} \tag{25}$$

In each of the different regions, one can again expand w.r.t. the appropriate parameters, for example:

$$\begin{aligned}&\int_{(ii)} \mathcal{T}_m\frac{1}{m^2+k^2}\frac{1}{m^2+(k-Q)^2} \approx \\ &\quad \int_{(ii)} \left(\mathcal{T}_m\frac{1}{m^2+k^2}\right)\left(\mathcal{T}_{m,k}\frac{1}{m^2+(k-Q)^2}\right) .\end{aligned} \tag{26}$$

Finally, for C one finds:

$$C = 2\int_{(i)\cup(ii)\cup(iii)} \left(\mathcal{T}_m\frac{1}{m^2+k^2}\right)\left(\mathcal{T}_{m,k}\frac{1}{m^2+(k-Q)^2}\right) , \tag{27}$$

which corresponds to massless tadpole integrals and therefore vanishes in dimensional regularization which we are using throughout.[2]

[2] I acknowledge a useful conversation with K. Melnikov on this issue.

The second term on the r.h.s. of Eq. (24) can be represented graphically as

$2\,\cdot$ 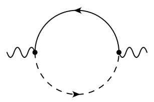 , (28)

meaning that the solid line should be expanded in all quantities but Q. Doing this, the actual integral will be of the tadpole type, with a more or less complicated vertex insertion. It is obtained from the original diagram by shrinking the solid lines shown in (28) to a point. In this sense, one can again use the diagrammatical equation (18) in order to represent Eq. (24). However, the interpretation is slightly different: In the second term, the diagram left of "$\star$" means the solid line of (28), and the one right of "$\star$" is the tadpole which remains when shrinking the expanded lines to a point. But the main difference between both interpretations of Eq. (18) is that according to Section 3.1 it is only valid up to terms of order $(m^2/q^2)^2$; according to Section 3.2, however, one may obtain the diagram to the r.h.s. up to arbitrary high powers in m^2/q^2 by pushing the Taylor expansions on the l.h.s. to sufficiently large order.

3.3. Large momentum and hard mass procedure [17, 22, 18, 23–25]

So far, two different viewpoints for the small-mass expansion of the polarization function have been presented. One is based on OPE and uses the language of quantum fields, while the second one examines the very Feynman *integrals*. The third viewpoint we will focus on is formulated mainly in terms of Feynman *diagrams*. Given a certain Feynman diagram with a particular distribution of masses and external momenta, the method generates a set of simpler diagrams which correspond to the asymptotic form of the original diagram in certain limits of the external parameters.

The particular case of a large external momentum as it was considered so far is usually referred to as "large momentum procedure". The opposite case of a mass being much larger than any other scale is called "hard mass procedure" and will be addressed below.

The prescription for the asymptotic expansion of Feynman diagrams can be summarized by the following formula [25]:

$$\mathcal{F}(\Gamma) \;\to\; \sum_\gamma \mathcal{F}(\Gamma\backslash\gamma) \;\star\; \mathcal{T}\mathcal{F}(\gamma)\,. \tag{29}$$

Here, Γ is the Feynman diagram under consideration, and $\mathcal{F}(\Gamma)$ is the corresponding Feynman integral. It shall contain either a set of large external momenta $\{Q\}$ or of large masses $\{M\}$. The arrow ($\to$) denotes that the r.h.s. is valid in the asymptotic limit of the M or Q going to infinity. The sum goes over all subgraphs γ of Γ that fulfill certain conditions to be described below. $\Gamma\backslash\gamma$ means the diagram that results when, within Γ, all lines of γ are shrunk to points. $\mathcal{T}$ means Taylor expansion w.r.t. all masses and external momenta that are *not* large. In particular, also those external momenta of γ that appear to be integration momenta in Γ have to be considered as small. The Taylor expansions are understood to be applied before any loop integrations are performed. In the following we will refer to the γ as *hard subgraphs* or simply *subgraphs*, to $\Gamma\backslash\gamma$ as the corresponding *co-subgraphs*. The "$\star$" means that $\mathcal{T}\mathcal{F}(\gamma)$ shall be inserted into $\mathcal{F}(\Gamma\backslash\gamma)$ at the point to which γ was contracted.

In other words: within Γ, all propagators of γ have to be expanded w.r.t. the masses and external momenta of γ that are not large.

3.3.1. Large momentum procedure

For the particular case of the large momentum procedure, the conditions that specify the hard subgraphs are as follows:

Every γ has to (i) contain all vertices where a large momentum enters or leaves the graph and (ii) be one-particle irreducible if these vertices were connected by an extra line.

As an example, consider again the one-loop diagram contributing to the photon polarization function, Fig. 1(a), in the limit of large external momentum. The set of hard subgraphs that emerge consists of three diagrams: first there is the diagram itself; the corresponding co-subgraph is just a point. The second subgraph is the one shown in (28) if the dashed line is omitted, and the third subgraph is the one symmetrical to that. The corresponding co-subgraphs are one-loop tadpole diagrams. In this way one again arrives at Eq. (18). The interpretation of the terms is the same as it was in the approach of Section 3.2.

As a two-loop example, let us examine the diagram shown in Fig. 1 (b):

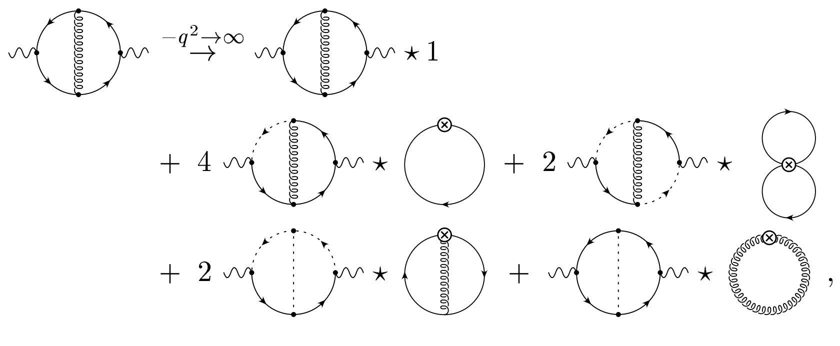

(30)

where the subgraphs are given by the solid lines of the diagrams left of "$\star$". The first term on the r.h.s. corresponds to the naive Taylor expansion. Note that the last diagram is zero in dimensional regularization.

It is interesting to relate this set of terms to the viewpoints of the previous section. In the operator language, the first term corresponds to the trivial operators $\mathbf{m}^{2n}$. The second one (actually only its m^4/q^4 contribution) is related to $C_{2,\mathrm{B}}\langle\mathcal{O}_2^{\mathrm{B}}\rangle$, the last one to $C_{1,\mathrm{B}}\langle\mathcal{O}_1^{\mathrm{B}}\rangle$. The other two terms, however, have no correspondence to any of the operators of Section 3.1. This is due to the fact that we considered only operators up to dimension four. But relation (30) is valid up to arbitrary orders in m^2/q^2. So the conclusion is that the third and fourth term on the l.h.s. are of order $(m^2/q^2)^3$ or higher.

The viewpoint described in Section 3.2, on the other hand, reproduces exactly the same terms as shown above.

3.3.2. Hard mass procedure

So far only the case of an external momentum being much larger than any other scale of the problem was considered. In this section the so-called hard mass procedure will be discussed. Here it is assumed that the diagram carries a mass that is much larger than all other masses and external momenta. Equation (29) remains valid, only the classification of the subgraphs is different. In the case of the hard mass procedure, γ must (i) contain all lines carrying a large mass (ii) be one-particle irreducible in its connected parts after contracting the heavy lines. Consider the following two-loop diagram as an example:

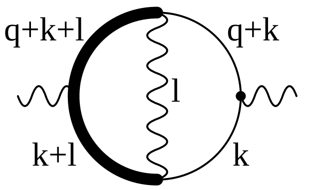

, (31)

where q is the external momentum flowing through the diagram from right to left. The mass of the thick line will be denoted by M. The imaginary part of (31) contributes to the electro-weak one-loop corrections of the process $Z \to b\bar{b}$ if top-quarks are attributed to the thick lines, b quarks to the plain thin lines, W bosons to the inner, and Z bosons to the outer wavy lines (see also Section 4 below). In the limit $q^2 \ll M^2$, the following subdiagrams emerge:

$$\begin{array}{l} k^2 \sim M^2 \\ l^2 \ \sim M^2 \end{array} : \qquad \begin{array}{l} k^2 \sim M^2 \\ l^2 \ll M^2 \end{array} : \qquad \begin{array}{l} k^2 \ll M^2 \\ l^2 \ \sim \ M^2 \end{array} : \qquad \begin{array}{l} k^2 \ll M^2 \\ l^2 \ll M^2 \end{array} :$$

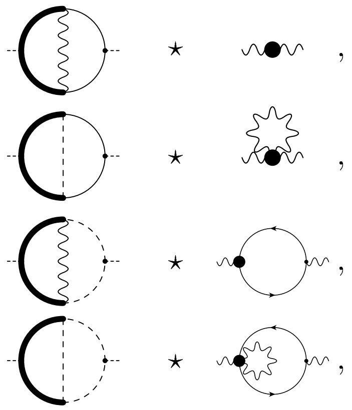

(32)

where we have indicated the region of loop momenta that generates the corresponding subdiagram according to the considerations or Section 3.2. It is again understood that the solid lines are to be expanded w.r.t. all external momenta and masses except M. The co-subgraphs, shown right of "$\star$", are obtained by contracting the solid lines to points.

3.3.3. Successive application of large momentum and hard mass procedure

In theories with many different particles of various masses, a realistic process generally involves several scales. The successive application of the large momentum and the hard mass procedure can be used to reduce any Feynman diagram to single-scale factors in this case, as long as a hierarchy among the different scales can be defined. This strategy was followed, for example, in the calculation of the anomalous magnetic moment of the muon [26], and later, using an automated setup, to the decay of the Z boson into b quarks [27] (see Section 4 below).

3.4. Expansions in other limits and range of applicability

Two concluding remarks shall be made to complete this formal section. First it should be noted that asymptotic expansions have been developed for various limiting cases (see, e.g., [28,20]). Only the two most straightforward ones have been described above. Other situations arise, for example, if the external momentum is either close to a mass or a threshold of the diagram. It appears that the most convenient way to formulate these expansions is in terms of the language of Section 3.2. Applications will be discussed briefly in the next Section.

The second remark that should be made concerns the applicability of asymptotic expansions, or in other words, the convergence properties of the series. By investigating the global structure of the problem, one often can read off regions of convergence for the function to be approximated. These regions may extend to values of the expansion parameter that are way beyond the initially required conditions.

Restrictions on the region of convergence, on the other hand, are mostly induced by the presence of thresholds. Thus, it often appears that with increasing number of loops the range of validity for the result decreases due to additional thresholds that are absent at lower order of perturbation theory.

4. Asymptotic expansions in practical applications

$R(s)$ to $\mathcal{O}(\alpha_s^2)$: in [29] the method of Section 3.3.1 was directly applied to the three-loop polarization function. For this purpose, the diagrammatical prescriptions were implemented in a computer program, called `lmp` [30], in order to cope with the large number of subdiagrams that had to be generated. For details on the calculation and the discussion of the results and their convergence properties we refer to [29, 31].

RG functions in MOM scheme: the large momentum procedure was also used to evaluate the relations between the renormalization constants of QCD in the $\overline{\rm MS}$ scheme to the ones in other schemes, in particular the MOM scheme, at $\mathcal{O}(\alpha_s^3)$. See [32] for more details.

$Z \to b\bar{b}$ to order $G_{\rm F}\alpha_s$: a sample diagram whose imaginary part contributes at $\mathcal{O}(G_{\rm F})$ is shown in Eq. (31). At order $G_{\rm F}\alpha_s$, an additional gluon has to be attached. One can apply the hard mass procedure w.r.t. M_t in this case, and it turns out that the leading term is proportional to M_t^2 due to the large mass splitting between the bottom and the top quark. There are two other scales in the problem, M_W and M_Z. In [27] they were factorized by a successive application of the hard mass procedure according to $M_W \gg M_Z$, an inequality whose use clearly has to be justified (see [27, 33]). The whole calculation would not have been possible without the computer program `EXP` [34]. As compared to `lmp`, it also performs the hard mass procedure and its combination with the large momentum procedure. Meanwhile the results of [27] have been confirmed by a different approach [35].

$t \to bW$ to $\mathcal{O}(\alpha_s^2)$: the problem here is that the contributing three-loop diagrams are actually on-shell, $q^2 = M_t^2$. Two different methods have been used to compute this process: The first calculation [36] used asymptotic expansions in the limit $1 - M_b^2/M_t^2 \ll 1$, the second one [37] evaluated the off-shell diagrams for $q^2 \ll M_t^2$ with the help of the hard mass procedure, taking the limit $q^2 \to M_t^2$ after performing a Padé approximation (see [37, 38] for details). The perfect agreement and the fairly high accuracy of the results in both approaches is a clear demonstration of the power of asymptotic expansions.

$\boldsymbol{e^+e^\Gamma \to t\bar{t}}$ **near threshold:** the development of asymptotic expansions in the threshold limit allowed to compute this process up to $\mathcal{O}(v^2, \alpha_s v, \alpha_s^2)$ [39], where v is the velocity of the top quarks in the cms system. It turned out that the corrections are huge and exhibit a strong dependence on the renormalization scale. The interpretation of this result and its implications are still an ongoing discussion (see [40] and references therein).

$\overline{\textbf{MS}}$ **to pole mass conversion at** $\boldsymbol{\mathcal{O}(\alpha_s^3)}$**:** among other things, the progress in threshold calculations mentioned above makes it very important to be able to express the $\overline{\rm MS}$ mass in terms of the pole mass at $\mathcal{O}(\alpha_s^3)$. The corresponding calculation of this relation was based on asymptotic expansions in the limit of small and large quark mass and interpolated the result for the actual on-shell diagrams with the help of Padé approximations [41].

$\boldsymbol{\mu}$ **decay and semileptonic** $\boldsymbol{b}$ **decays:** for special final state configurations the decay $b \to cl\bar{\nu}$ was computed up to $\mathcal{O}(\alpha_s^2)$ using asymptotic expansions in the limit $1 - M_c^2/M_b^2 \ll 1$ [42]. For $b \to ul\bar{\nu}$, the full inclusive result was obtained through a four-loop calculation, where the actual integrals were calculated by performing an asymptotic expansion and resumming the full series [43]. The same technique was applied to the 2-loop QED corrections to muon decay [44]. Using an approach similar to the one of [37] (see above), the results of [44, 43] were recently confirmed [45].

5. Back to OPE: RG improvement

The advantages of the approach of Sections 3.2 and 3.3 in comparison to the one of Section 3.1 when calculating Feynman diagrams are obvious: In the OPE language one needs to define a full set of operators for every order in m^2 and to apply the appropriate projectors in order to obtain the coefficient functions. Using the large momentum procedure, all operations can be performed on the level of Feynman diagrams. The depth of the expansion in m^2 is just a matter of evaluating the Taylor expansions to sufficiently high orders. However, the loss of contact to the quantum field theoretic level has its price. In this section two advantages of the OPE language over the strict application of the large momentum procedure will be described.

5.1. Resummation of logarithms [46]

Consider the expansion of the polarization function w.r.t. small m^2/q^2 (see Eq. (6)). The coefficients of this series contain logarithms of the form $\ln(\mu^2/m^2)$ and $\ln(-\mu^2/q^2)$. The former arise from the tadpole diagrams (in the OPE language: the vacuum expectation values; in the large momentum procedure: the co-subgraphs), the latter from the massless propagator diagrams (coefficient functions/hard subgraphs). Working at fixed order in perturbation theory, one has to choose some value for μ in order to make predictions for physical quantities. It is clear that one should choose μ such that the coefficients of the perturbative series are small. However, with the two types of logarithms above this might be impossible. In the OPE approach this problem can be solved in the following way: the operators fulfill the renormalization group (RG) equation

$$\mu^2 \frac{\mathrm{d}}{\mathrm{d}\mu^2} \mathcal{O}_n = \sum_n \gamma_{nm} \mathcal{O}_m \,, \tag{33}$$

where γ_{nm} is their anomalous dimension related to the renormalization matrix Z_{nm} of (13) by

$$\gamma_{nm} = \sum_k \left(\mu^2 \frac{\mathrm{d}}{\mathrm{d}\mu^2} Z_{mk} \right) (Z^{-1})_{kn} \,. \tag{34}$$

The solution of (33) is of the form

$$\mathcal{O}_n(\mu) = \sum_m R_{nm} \mathcal{O}_m(\mu_0) \,, \tag{35}$$

where R_{nm} depends on μ and μ_0 only implicitly through its dependence on α_s. One can now rewrite the OPE as

$$\Pi(q^2) = \sum_n C_n(\mu) \mathcal{O}_n(\mu) = \sum_{n,m} C_n(\mu) R_{nm} \mathcal{O}_m(\mu_0) \,. \tag{36}$$

Setting $\mu^2 = q^2$ and $\mu_0^2 = m^2$ removes both types of logarithms discussed above. Using the diagram-wise expansions of Sections 3.2 or 3.3, such kind of resummation is not possible in a straightforward way.

5.2. Reconstruction of higher orders in α_s

Consider the expansion of $\Pi(q^2)$ in small m^2/q^2 at $(l+1)$-loop level. It appears that the only proper $(l+1)$-loop diagrams that contribute arise from the naive Taylor expansion, or in other words, from the trivial operators $\mathbf{m}^{2n}$. All the additional terms are products of diagrams with a lower number of loops. In the following we will show that this fact allows to derive the physically relevant quantity $R = \mathrm{Im}\Pi$ at $(l+1)$-loop level from an l-loop calculation assuming the OPE approach of Section 3.1.

To be specific, consider the calculation of the m^4 terms of $\Pi(q^2)$. The dimension-4 piece of the OPE fulfills the following RG equation:

$$\mu^2 \frac{\mathrm{d}}{\mathrm{d}\mu^2} \sum_{n=1}^{3} C_n \mathcal{O}_n = 0\,. \tag{37}$$

The effect of the derivative on the $\mathcal{O}_n$ is again determined by (33). On the other hand, because the C_n do not depend on masses, we can write

$$\mu^2 \frac{\mathrm{d}}{\mathrm{d}\mu^2} C_n = \left(\frac{\partial}{\partial L} + \alpha_s \beta \frac{\partial}{\partial \alpha_s}\right) C_n\,, \tag{38}$$

where $L = \ln(-\mu^2/q^2)$. Inserting this into (37), collecting the coefficients of $\mathcal{O}_3$ and using $\gamma_{33} = 4\gamma^m$ (this can be seen by recalling $\mu^2 \frac{\mathrm{d}}{\mathrm{d}\mu^2} m = \gamma^m m$), one obtains [16]:

$$\frac{\partial}{\partial L} C_3 = -4\gamma^m C_3 - \alpha_s \beta \frac{\partial}{\partial \alpha_s} C_3 - \sum_{n=1,2} \gamma_{n3} C_n\,. \tag{39}$$

Performing an l-loop calculation, C_1 and C_2 are known to order α_s^l, C_3 only to α_s^{l-1}. But since β and γ^m do not contain terms of order α_s^0, the r.h.s. is known to $\mathcal{O}(\alpha_s^l)$ (assuming that the anomalous dimensions are known to appropriate order), and so is the l.h.s. The logarithmic terms (and thus the desired imaginary part) of C_3 can therefore be obtained to $\mathcal{O}(\alpha_s^l)$ by trivial integration.

This strategy was first followed in [16] to derive the $m^4\alpha_s^2$ terms of $R(s)$. The extension to $m^4\alpha_s^3$ was performed in [47] (see also [48]).

6. Conclusions

In this lecture we have discussed the methods for asymptotic expansions of Feynman integrals. The field theoretical approach via operator product expansion has been compared to the diagram-wise methods, and the advantages of both strategies have been outlined. We hope that the importance of the numerous applications — we could sketch only a few of them — has convinced the reader of the power and flexibility of these expansions.

Acknowledgments

I would like to thank K.G. Chetyrkin, J.H. Kühn, T. Seidensticker, and M. Steinhauser for fruitful collaboration on various topics and careful reading of the manuscript. I am indebted to A. Czarnecki, K. Melnikov, and

A. Rétey for several enlightening discussions and useful comments on the text. I would further like to thank the organizers of the school for the invitation and the pleasant atmosphere. This work was supported by the *Deutsche Forschungsgemeinschaft*.

REFERENCES

[1] T. Hahn, these proceedings.

[2] R. Harlander and M. Steinhauser, *Prog. Part. Nucl. Phys.* **43** (1999) 167.

[3] G. Degrassi, P. Gambino, and A. Sirlin, *Phys. Lett.* **B 383** (1996) 219; G. Degrassi, P. Gambino, and A. Sirlin, *Phys. Lett.* **B 394** (1997) 188; G. Degrassi, P. Gambino, M. Passera, and A. Sirlin, *Phys. Lett.* **B 418** (1998) 209; S. Bauberger and G. Weiglein, *Phys. Lett.* **B 419** (1998) 333.

[4] K.G. Chetyrkin and F.V. Tkachov, *Nucl. Phys.* **B 192** (1981) 159; F.V. Tkachov, *Phys. Lett.* **B 100** (1981) 65.

[5] D.J. Broadhurst, *Z. Phys.* **C 54** (1992) 599.

[6] L.V. Avdeev, *Comp. Phys. Commun.* **98** (1996) 15.

[7] S.A. Larin, F.V. Tkachov, and J.A.M. Vermaseren, Report No. NIKHEF-H/91-18 (Amsterdam, 1991).

[8] M. Steinhauser, Dissertation, University of Karlsruhe (Shaker Verlag, Aachen, 1996).

[9] K.G. Chetyrkin, J.H. Kühn and A. Kwiatkowski, *Phys. Reports* **277** (1997) 189.

[10] K.G. Chetyrkin, J.H. Kühn and M. Steinhauser, *Phys. Lett.* **B 371** (1996) 93; *Nucl. Phys.* **B 482** (1996) 213.

[11] R. Rückl, these proceedings.

[12] V.P. Spiridonov, Rep. No. INR P-0378 (Moscow, 1984); K.G. Chetyrkin and V.P. Spiridonov, *Yad. Fiz.* **47** (1988) 818 (*Sov. J. Nucl. Phys.* **47** (1988) 522).

[13] T. van Ritbergen, J.A.M. Vermaseren, and S.A. Larin, *Phys. Lett.* **B 400** (1997) 379.

[14] K.G. Chetyrkin, *Phys. Lett.* **B 404** (1997) 161;
J.A.M. Vermaseren, S.A. Larin, and T. van Ritbergen, *Phys. Lett.* **B 404** (1997) 153.

[15] K.G. Chetyrkin, private communication.

[16] K.G. Chetyrkin and J.H. Kühn, *Nucl. Phys.* **B 432** (1994) 337.

[17] K.G. Chetyrkin, S.G. Gorishny, and F.V. Tkachov, *Phys. Lett.* **B 119** (1982) 407.

[18] S.G. Gorishny and S.A. Larin, *Nucl. Phys.* **B 283** (1987) 452.

[19] L.R. Surguladze and F.V. Tkachov, *Nucl. Phys.* **B 331** (1990) 35.

[20] M. Beneke and V.A. Smirnov, *Nucl. Phys.* **B 522** (1998) 321.

[21] V.A. Smirnov, hep-ph/9907471.

[22] G.B. Pivovarov, F.V. Tkachov, Rep. No. INR P-0370 (Moscow, 1984);
F.V. Tkachov, *Int. Journ. Mod. Phys.* **A 8** (1993) 2047;
G.B. Pivovarov, F.V. Tkachov, *Int. Journ. Mod. Phys.* **A 8** (1993) 2241.

[23] K.G. Chetyrkin,V.A. Smirnov, Rep. No. INR P-518 (Moscow, 1987);
K.G. Chetyrkin, *Theor. Math. Phys.* **75** (1988) 346 and ibid. **76** (1988) 809;
V.A. Smirnov, *Comm. Math. Phys.* **134** (1990) 109.

[24] S.G. Gorishny, *Nucl. Phys.* **B 319** (1989) 633.

[25] V.A. Smirnov, *Renormalization and Asymptotic Expansion* (Birkhäuser, Basel, 1991); *Mod. Phys. Lett.* **A 10** (1995) 1485.

[26] A. Czarnecki, B. Krause, and W.J. Marciano, *Phys. Rev. Lett.* **76** (1996) 3267;
A. Czarnecki and B. Krause, *Phys. Rev. Lett.* **78** (1997) 4339.

[27] R. Harlander, T. Seidensticker, and M. Steinhauser, *Phys. Lett.* **B 426** (1998) 125.

[28] V.A. Smirnov, *Phys. Lett.* **B 394** (1997) 205; A. Czarnecki and V.A. Smirnov, *Phys. Lett.* **B 394** (1997) 211.

[29] K.G. Chetyrkin, R. Harlander, J.H. Kühn and M. Steinhauser, *Nucl. Phys.* **B 503** (1997) 339.

[30] R. Harlander, Dissertation, University of Karlsruhe (Shaker Verlag, Aachen, 1998).

[31] K.G. Chetyrkin, R. Harlander, J.H. Kühn and M. Steinhauser, *Nucl. Inst. Meth.* **A 389** (1997) 354.

[32] K.G. Chetyrkin and A. Rétey, Karlsruhe TTP99-43, hep-ph/9910332; see also these proceedings.

[33] R. Harlander, *Act. Phys. Pol.* **B 29** (1998) 2691.

[34] T. Seidensticker, Diploma Thesis, University of Karlsruhe (unpublished).

[35] J. Fleischer, F. Jegerlehner, M. Tentyukov, and O. Veretin, *Phys. Lett.* **B 459** (1999) 625.

[36] A. Czarnecki and K. Melnikov, *Nucl. Phys.* **B 544** (1999) 520.

[37] K.G. Chetyrkin, R. Harlander, T. Seidensticker, and M. Steinhauser, hep-ph/9906273, *Phys. Rev.* **D** (in print).

[38] K.G. Chetyrkin, R. Harlander, T. Seidensticker, and M. Steinhauser, *Proc. Europhysics Conf. EPS-HEP99, Tampere, Finland, 1999*, hep-ph/9910339.

[39] A.H. Hoang and T. Teubner, *Phys. Rev.* **D 58** (1998) 114023;
K. Melnikov and A. Yelkhovsky, *Nucl. Phys.* **B 528** (1998) 59;
M. Beneke, A. Signer, and V.A. Smirnov, *Phys. Lett.* **B 454** (1999) 137.

[40] M. Jeżabek, these proceedings.

[41] K.G. Chetyrkin and M. Steinhauser, hep-ph/9907509, *Phys. Rev. Lett.* (in print).

[42] A. Czarnecki, *Phys. Rev. Lett.* **76** (1996) 4124;
A. Czarnecki and K. Melnikov, *Phys. Rev. Lett.* **78** (1997) 3630; *Nucl. Phys.* **B 505** (1997) 65; *Phys. Rev.* **D 59** (1999) 014036;
J. Franzkowski and J.B. Tausk, *Eur. Phys. J.* **C 5** (1998) 517.

[43] T. van Ritbergen, *Phys. Lett.* **B 454** (1999) 353.

[44] T. van Ritbergen and R. G. Stuart, *Phys. Rev. Lett.* **82** (1999) 488.

[45] T. Seidensticker and M. Steinhauser, hep-ph/9909436, *Phys. Lett.* **B** (in print).

[46] K.G. Chetyrkin, C.A. Dominguez, D. Pirjol, and K. Schilcher, *Phys. Rev.* **D 51** (1995) 5090.

[47] K.G. Chetyrkin, R. Harlander, and J.H. Kühn, in preparation.

[48] K.G. Chetyrkin, R. Harlander, and J.H. Kühn, *Proc. Europhysics Conf. EPS-HEP99, Tampere, Finland, 1999*, hep-ph/9910345.